Chemosphere 144 (2016) 1682–1689

Contents lists available at ScienceDirect

Chemosphere

journal homepage: www.elsevier.com/locate/chemosphere

The dual effects of carboxymethyl cellulose on the colloidal stability and toxicity of nanoscale zero-valent iron

Haoran Dong [a, b, *], Yankai Xie [a, b], Guangming Zeng [a, b], Lin Tang [a, b], Jie Liang [a, b], Qi He [a, b], Feng Zhao [a, b], Yalan Zeng [a, b], Yanan Wu [a, b]

[a] College of Environmental Science and Engineering, Hunan University, Changsha, Hunan 410082, China
[b] Key Laboratory of Environmental Biology and Pollution Control (Hunan University), Ministry of Education, Changsha, Hunan 410082, China

HIGHLIGHTS

- The dual effects of CMC on the stability and cytotoxicity of NZVI were investigated.
- The CMC-coating significantly reduced the cytotoxicity of NZVI towards *Echerichia coli*.
- The Ca^{2+} can either increase or decrease the cytotoxicity of NZVI and CMC-NZVI.
- The cytotoxicity of NZVI and CMC-NZVI significantly decreased after aging.
- The mechanisms related to the particle stabilization and toxicity were discussed.

GRAPHICAL ABSTRACT

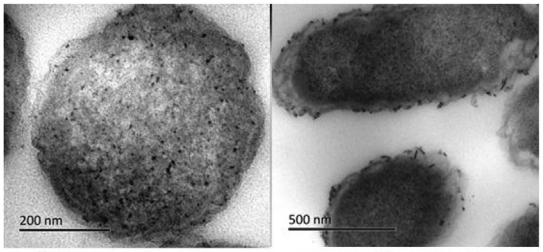

ARTICLE INFO

Article history:
Received 6 September 2015
Received in revised form
7 October 2015
Accepted 15 October 2015
Available online xxx

Keywords:
Aging
Carboxymethyl cellulose
Colloidal stability
Escherichia coli
Nanoscale zero-valent iron
Toxicity

ABSTRACT

Nanoscale zero-valent iron (NZVI) particles are usually modified with surface coating to mitigate the particle stability in water during the environmental application. However, the surface coating may not only influence the particle stabilization but also the particle cytotoxicity. In this study, we investigated the dual effects of carboxymethyl cellulose (CMC) on the colloidal stability and cytotoxicity of NZVI towards gram-negative *Escherichia coli* (*E. coli*) and discussed the interrelation between particle stability and cytotoxicity. The effect of CMC concentration, ionic strength (Ca^{2+}) and aging treatment on the particle cytotoxicity were also examined. Specifically, the aqueous stability of NZVI suspensions with CMC ratio dose-dependently strengthened within 1 h. The inactivation of *E. coli* by bare NZVI was significant and concentration- and time-dependent. On the contrary, an increasing reduction in cytotoxicity of NZVI with CMC ratio increasing was observed, even though the particles became more dispersed. TEM analysis demonstrates the membrane disruption and the cellular internalization of nanoparticles after exposure of *E. coli* to NZVI. However, in the case of CMC-modified NZVI (CNZVI), the bacterial cell wall displays an outer shell of a layer of nanoparticles attached around the outer membrane, but the cell membrane was kept intact. The presence of Ca^{2+} can either increase or decrease the cytotoxicity of NZVI and CNZVI, depending on the concentration. The aged NZVI and CNZVI particles did not seem to present obvious bactericidal effect due to the transformation of Fe^0 to the less toxic or non-toxic iron oxides, as indicated by the XRD analysis.

* Corresponding author. College of Environmental Science and Engineering, Hunan University, Changsha, Hunan 410082, China.
E-mail address: dongh@hnu.edu.cn (H. Dong).

http://dx.doi.org/10.1016/j.chemosphere.2015.10.066
0045-6535/

1. Introduction

Nanoscale zero-valent iron (NZVI) particles have been prevalently used to treat inorganic salt (e.g., NO_3^-), chlorinated organic pollutants (e.g., TCE) and heavy metals (e.g., Cr(VI)) by injecting the NZVI particles into the subsurface where has been contaminated (Kanel et al., 2006; Lowry, 2007; Ramos et al., 2009). While the use and development of NZVI are understandably heralded as a promising environmental nanotechnology, the long-term stability and potential health and environmental risk of NZVI during the course of treatment has not been solved properly (Dong et al., 2012, 2015; Grieger et al., 2010; Phenrat et al., 2009).

It has been reported that bare NZVI particles aggregate rapidly in water, making subsurface delivery difficult (Kanel et al., 2007; Liu et al., 2015; Phenrat et al., 2007). In order to decrease aggregation and enhance the mobility of NZVI, surface stabilizers (e.g., polyelectrolyte, surfactant, biopolymer) can be coated onto the surface of the particles to provide electrostatic repulsion, and steric or electrosteric stabilization (Saleh et al., 2008; Sirk et al., 2009; Fatisson et al., 2010; Dong and Lo, 2013a). Various surface coatings, such as anionic or nonionic surfactants (Kanel et al., 2007; Saleh et al., 2008), poly propionate (Jiemvarangkul et al., 2011), starch (He and Zhao, 2005), carboxymethyl cellulose (CMC) (He et al., 2007; Raychoudhury et al., 2012) and guar gum (Tiraferri et al., 2008), have been investigated to stabilize the NZVI particles and the results are promising. However, the stability of the nanoparticles also depends on the geochemical characteristics of groundwater (e.g., ionic strength) (He and Zhao, 2005; He et al., 2007; Saleh et al., 2008). It was found that electrostatic stabilization, provided by the coating of charged polymers or surfactants, is sensitive to ionic strength, and hence unlikely to be effective (Dong and Lo, 2014). In the case of polyelectrolyte surface coatings (e.g., CMC), so-called steric or electrosteric stabilization provides good resistance to changing electrolyte conditions likely to be encountered in real groundwater (Dong and Lo, 2013b; He et al., 2007; Raychoudhury et al., 2012).

Although NZVI has become the most potential nanomaterials for soil and groundwater remediation, it is confronted with query about the negative effect of eco-environment in environment remediation application (Grieger et al., 2010; Karn et al., 2009; Lee et al., 2008). Lee et al. (2008) found that exposure of *Escherichia coli* (*E. coli*) to NZVI lead to the disruption of cytomembrane and leakage of intracellular substances, whereas oxidized nanoparticles, microscale zero-valent iron and ferric ions had no apparent cytotoxicity. Li et al. (2010) indicated that the adsorbed polymer and natural organic matter limited adhesion and toxicity of NZVI to *E. coli* and aged NZVI without Fe^0 eliminated its bactericidal effects. Chen et al. (2011a,b, 2013) reported that CMC-stabilized NZVI and Fe(II) solutions caused acute lethally and sublethally toxic effects in medaka larvae, while its oxidation products (Fe_3O_4) caused the least toxic effects. However, Zhou et al. (2014) suggested that CMC-NZVI emerged minimized oxidative stress response and tardier disruption of cell wall integrity, which led to less toxicity effects to bacteria Agrobacterium sp. PH-08 than bare NZVI.

As discussed above, the surface coatings may not only influence the colloidal stability but also exert effects on the cytotoxicity of NZVI particles. Given the finding that the NZVI particles are more toxic than the microscale ZVI (Li et al., 2010), there is a growing concern that the more dispersed NZVI particles after surface modification may exert more toxic effects than the bare NZVI particle (which may aggregate to micron-size). However, to date, most of studies focused on the individual effect of surface coating on the colloidal stability or the toxicity of surface-modified NZVI (Dong and Lo, 2013a; Tang and Lo, 2013), no studies have systematically examined the dual effects of surface coating with both the colloidal stability and the toxicity of NZVI taken into account. The objectives of this study are (1) to investigate the dual effect of surface coating on the colloidal stability and toxicity of NZVI towards *E. coli* and 2) to probe into the effects of surface coating concentration, electrolytes in groundwater and aging time of NZVI on the toxic effect of surface-modified NZVI. NZVI modified with carboxymethyl cellulose (CMC, one type of polyelectrolyte) was employed in this study. The chosen surface stabilizer is reported to provide the steric or electrosteric stabilization, and proved to be highly effective in typical groundwater ionic strength (He et al., 2007; Raychoudhury et al., 2012).

2. Materials and methods

2.1. Chemical reagents

NaCl, $CaCl_2 \cdot 6H_2O$ were purchased from Damao Chemical Reagent Factory (Tianjin). Tryptone, Yeast Extract, Eosin-methylene Blue Agar (EMB) were purchased from ShengSi biochemical technology co. (Shanghai). Carboxymethyl cellulose (CMC, MW = 90,000) were purchased from Jingkang new material technology co. (Changsha). All reagents for experiments were of reagent grade and used without further purification. All solutions and dilutions were prepared in ultrapure water (Barnstead D11911). Ultrapure water was purged with nitrogen gas for 1 h prior to usage.

2.2. Preparation of NZVI and CMC-modified NZVI

Nanofer 25 NZVI particles (produced from nanosized ferrihydrite) in aqueous dispersion form were graciously supplied by the NANOIRON® Company (Czech Republic, EU). Concentration units were presented as "ppm" in keeping with toxicity nomenclature (1 ppm = 1 mg L^{-1}). Nanofer 25 (referred to as NZVI in this study) was diluted with N_2 saturated ultrapure water to three concentrations (100, 300, 500 ppm) and ultrasonicated for 30 min to ensure the uniform dispersion. NZVI was used for further modification by using CMC. CMC-modified NZVI is referred to as CNZVI in the following. CNZVI was prepared by dispersing NZVI particles in aqueous CMC to result in suspensions comprising iron nanoparticles (500 ppm) and CMC of various concentrations (0, 0.01, 0.02, 0.03, 0.05, 0.1, 0.4, 0.8, 1.2, 1.6 wt%) individually, followed by sonication for 30 min.

2.3. Measuring the sedimentation of iron nanoparticles

The sedimentation kinetics of CNZVI was determined for various CMC concentrations by monitoring the optical absorbance at 508 nm by UV–vis spectrophotometry (UV-2550, SHIMADZU, Japan) in a drive-time mode for 1 h. All measurements were made at 25 °C in duplicate. The solution pH (~7.5) of CNZVI was measured by a pH meter (INESA, PHS-3C). Surface charges of NZVI before and after surface modification were measured with a zeta potential analyzer (Nano-ZS90, Malvern).

2.4. E. coli culture

E. coli (ATCC 25922) was purchased from the China Center for 173 Type Culture Collection (Beijing, China). Preculture of the strain was performed in Luria-Bertani (LB) medium containing 5 g L^{-1} of yeast extract, 10 g L^{-1} of tryptone and 5 g L^{-1} of NaCl. Cultures were inoculated from precultures in 60 mL LB Broth and grown at 37 °C for 12 h. The bacteria were harvested by centrifugation at 5000 g for 10 min. The supernatant was removed, and the cells were

resuspended in a 9 g L^{-1} NaCl solution (sterile normal saline) and then centrifuged again at 5000 g for 10 min. This washing step was repeated once. The *E. coli* stock was prepared by resuspending the bacteria pellets in 30 mL of sterile normal saline. The stock concentration of *E. coli* ranged over 1×10^9 to 2×10^9 colony forming units (CFU)/mL by the spread plate method using EMB incubated at 37 °C for 18 h.

2.5. Toxicity assessments

For the inactivation experiments, *E. coli* was incubated with NZVI or CNZVI suspensions. The suspensions were added in 50 mL culture tubes to supply an ultimate concentration of 500 ppm. The assessments were conducted under anaerobic conditions with the tubes sealed at room temperature (21 ± 0.5 °C) requiring a *E. coli* concentration of 10^6 CFU/mL, prepared by diluting *E. coli* stock in 20 mL particle suspensions. The culture tubes were placed on a shaking incubator at 300 rpm, sampling at 0, 5, 15, 30, 45 and 60 min and serially diluted with sterile normal saline. The cells were plated on EMB incubated at 37 °C for 18 h, and then counted (Li et al., 2010).

In order to determine the influence of Ca^{2+} on the toxicity of iron nanoparticles towards *E. coli*, the NZVI or CNZVI solutions (500 ppm) containing Ca^{2+} (10 ppm and 40 ppm) were prepared by adding Ca^{2+} into the iron nanoparticle suspension. Toxicity assessments were conducted subsequently according to the same procedure as mentioned above.

To assess the effect of iron oxidation ("aging") on the toxicity of iron nanoparticles, *E. coli* was exposed to the aged iron nanoparticles, which were prepared by settling the NZVI or CNZVI suspensions (500 ppm) for 15 d and 30 d under static water in an open tube. X-ray diffraction (XRD) analysis for the aged iron nanoparticles was obtained using Cu Kα radiation on a MXP18 HF diffractometer (MAC Science Co., Japan).

2.6. Transmission Electron Microscopy (TEM) analysis of E. coli cells

E. coli cells were exposed to 500 ppm of iron nanoparticles for 1 h. To forestall adhesion of bacteria onto NZVI, the NZVI particles (which are magnetic (Phenrat et al., 2007)) were removed prior to cell collection using a commercial magnet placed at the bottom of the sample tube. The supernatant was decanted into another tube, and cells were then gathered by centrifugation (5000 g at 4 °C for 10 min), repeated this washing step for twice (Xiu et al., 2010a). The native and treated cells were fixed in 2.5% glutaraldehyde and 0.01 M phosphate buffer for 2 h, followed by washing three times with 0.01 M phosphate buffer and postfixing with 1% osmic acid fixative for 2 h. The washing step was repeated again. Then the cells were dehydrated with sequential treatment with 50, 70, 90, and 100% acetone for 15 min. The cells were then infiltrated in embedding agent and pure acetone (treatment with 1:1 of embedding agent/pure acetone mixtures for 12 h, and embedding agent for 12 h at 37 °C). The samples were cured overnight at 37 °C and 60 °C for 12 h to form sample blocks. The blocks were sectioned for 50–100 nm using an ultramicrotome, and the thin sections were stained in 3% uranyl acetate and lead citrate and examined by TEM (FEI Tecnai G2 Spirit).

3. Results and discussion

3.1. Aqueous stability of iron nanoparticles

The colloidal stability of iron nanoparticles was investigated by monitoring the sedimentation kinetics of nanoparticle dispersions (Fig. 1). As shown in Fig. 1, a significant and rapid sedimentation was observed at the outset of the experiment for the bare NZVI without surface modification, and an even faster settling was observed after 10 min. This is in consistence with the previous studies (Yin et al., 2012; Dong and Lo, 2013a), which have indicated that the settlement of NZVI may follow two concomitant processes: (1) direct sedimentation of some particles with larger size, and (2) aggregation of the residual particles with smaller size followed by sedimentation. While the CMC-modified NZVI (CNZVI) displayed a lower degree of settling and the settling of CNZVI was less significant with increasing concentration of CMC from 0.4 wt% to 1.6 wt% (Fig. 1). Previous analysis of the electrokinetic data along with QCM-D results suggested that electrosteric repulsion can play a noted role in NZVI colloid stabilization by CMC (Fatisson et al., 2010; Chen et al., 2013). Dong and Lo (2013a) also reported that the polyelectrolytes slow deposition of the particles by reducing the magnetic attraction of the NZVI to each other due to the electrostatic repulsion effect. The zeta potential of bare NZVI and CNZVI were measured and the results show that the presence of CMC significantly increased the negative charge of NZVI surface (Table 1). The distinction of zeta potentials between NZVI and CNZVI indicates the successful CMC coating on the surface of NZVI and meanwhile CNZVI had higher stable dispersal potency than NZVI. Additionally, it was interesting to observe that the negative charge of CNZVI increased with the increasing concentration of CMC from 0.03 wt% to 0.4 wt %, while it did not increase further with the increase in the concentration of CMC but decreased to some degree. Lin et al. (2010) reported that the coating of polyacrylic acid (PAA) on the surface of NZVI and found that the PAA was not only adsorbed on the NZVI surface in the structure of bidentate bridging, but also formed a gel network through hydrogen bonding, PAA entanglement and PAA cross-linking. Consequently, there are few free carboxylic groups on the surface of PAA-modified NZVI. Therefore, it was presumed that the decrease in negative surface charge with the increasing concentration of CMC might be ascribed to the entanglement or cross-linking of the CMC molecules on the surface of CNZVI. However, even though the negative surface charge of CNZVI decreased when the concentration of CMC was larger than 0.4 wt%, the CNZVI particles became more stable with increasing CMC concentration from 0.4 wt% to 1.6 wt%. This indicates that the steric effect played an important role in stabilizing the CNZVI particles.

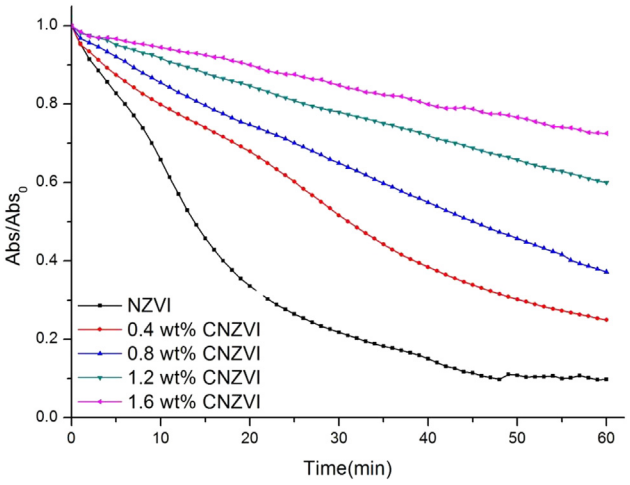

Fig. 1. Sedimentation kinetics of NZVI and CNZVI with different CMC concentrations (Concentration of NZVI or CNZVI: 500 mg L^{-1}).

Table 1
Zeta potential (mV) for NZVI and CNZVI with various CMC concentrations w/o Ca^{2+} at pH 7.5. (Results are the average of triplicate experiments).

Ca^{2+} (mg L^{-1})	CMC (wt%)						
	0	0.03	0.05	0.4	0.8	1.2	1.6
0	−20.1	−44.6	−49.2	−61.5	−43.4	−50.6	−49.4
10	−4.7	−36.9	_	−50.8	_	_	_
40	4.4	−25	_	−47.9	_	_	_

3.2. Effects of iron nanoparticles on cell viability of *E. coli*

The bactericidal effects of NZVI and CNZVI nanoparticles towards *E. coli* were investigated. The *E. coli* inactivation was expressed as $\log(N/N_0)$, where N and N_0 are the remaining and initial numbers of viable *E. coli* cells (CFU/mL), respectively. The results of the survival tests for the *E. coli* in the presence of NZVI with a concentration gradient are shown in Fig. 2a, which shows that the inactivation of *E. coli* by NZVI was concentration- and time-dependent. Exposure to 100 ppm of NZVI under anaerobic conditions resulted in an approximate 0.5-log reduction in viable *E. coli* cells after 30 min and up to nearly 0.7-log reduction in viable *E. coli* cells after 1 h. The increasing concentration of NZVI exerted more serious toxicity towards *E. coli*. At 500 ppm of NZVI, 1.1- and 2.9-log reductions in viable *E. coli* cells were observed after 30 min and 1 h, respectively. Previous studies have shown that both Fe^0 content and the presence of dissolved Fe(II) have been positively correlated with NZVI toxicity to *E. coli* (Auffan et al., 2008; Lee et al., 2008). Besides, the NZVI has been shown to generate reactive oxygen species (ROS) such as hydroxyl radicals (·OH) that may be toxic to *E. coli* (Joo et al., 2005). Thus the NZVI of high concentration has more Fe^0, produces more Fe(II) and ROS which may inactivate the cells faster than that of the low concentrations (Lee et al., 2008).

The toxicity of CNZVI (NZVI modified with CMC of various concentrations from 0.01 to 1.6 wt%) at 500 ppm was examined and compared with that of bare NZVI (Fig. 2b). It was found that although the presence of 0.01 wt% CMC slightly decreased the toxicity of CNZVI, the presence of 0.03 wt% CMC significantly reduced the toxicity of CNZVI (only 1.5-log reductions in viable *E. coli* cells after 1 h). The increasing concentration of CMC from 0.1 wt% to 1.6 wt% resulted in less than a 0.2-log reduction in viable *E. coli* cells. Evidently, CMC-coating significantly reduced the cytotoxicity of NZVI towards *E. coli*. To make sure that this toxicity is related to the iron nanoparticles themselves and not to the presence of remnant from the modification, the toxicity of the CMC (1.6 wt%, the maximum concentration used to synthesize CNZVI herein) was evaluated. The inactivation of *E. coli* in CMC-containing solution was negligible after 1 h (<0.1-log, Fig. 2b), indicating that the CMC, which may be released from the surface of CNZVI, do not cause the *E. coli* inactivation. In other words, no toxicity of CMC was observed, confirming that the toxic effect arose from iron nanoparticles alone. There was much evidence suggesting that NZVI induced intracellular oxidative stress, leading to cell death (Chen et al., 2011a, 2011b, 2012; Fajardo et al., 2013; Sacca et al., 2014, 2013; Xiu et al., 2010b; Zhou et al., 2014). With the addition of NZVI to bacteria, the redox-active Fe^{2+} concentration increased, which then would trigger intracellular oxidative stress via Fenton chemistry (Ševců et al., 2011). The toxic process of NZVI seemed to be similar to Ag and CuO nanoparticles in some degree, which govern their toxicity by dissolved fractions of their nanoparticles (Jo et al., 2012). Oxygenation of reduced Fe species (Fe^{2+} and/or Fe^0) are known to be competent ROS producer (Eqs (1)–(3)). ROS can be straightly generated due to oxidation of Fe^{2+} during the erosion of NZVI via the Fenton reaction or from configurational Fe^{2+} at the

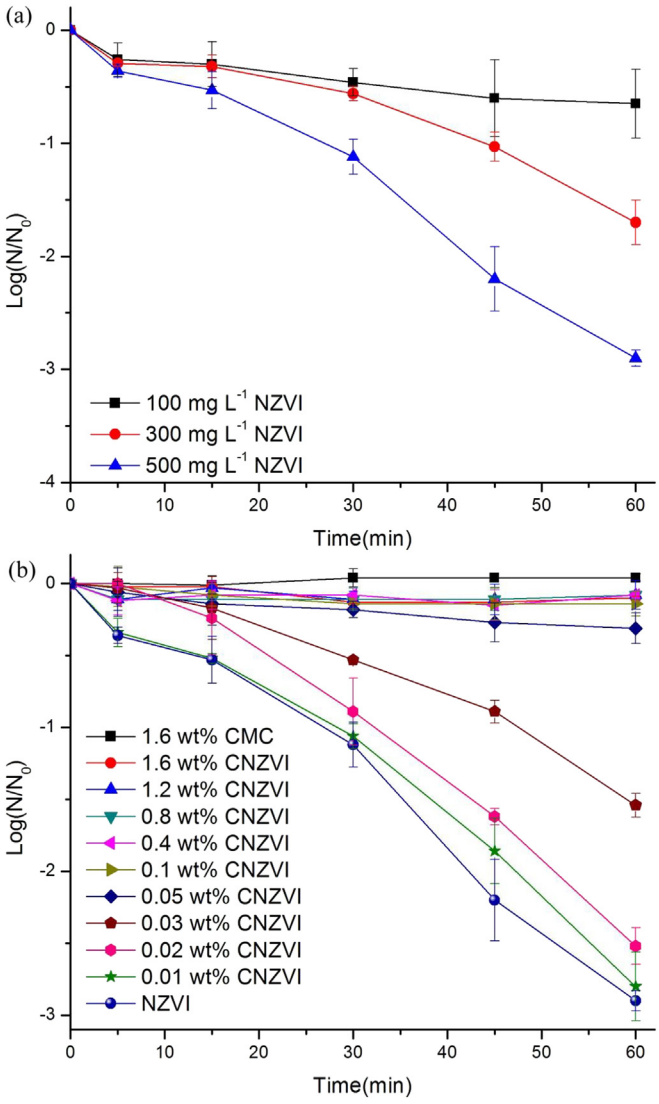

Fig. 2. Exposure of *E. coli* to (a) NZVI of different concentrations for 1 h; (b) NZVI and CNZVI of various CMC concentrations (Concentration of NZVI or CNZVI: 500 mg L^{-1}).

Fe_3O_4 surface, even interior Fe^{2+} of magnetite released to solution (Joo et al., 2005; Schoonen et al., 2006). Also, NZVI are capable of facilitating this reaction via Eq (2) and generate Fe^{2+} in another way again (Auffan et al., 2008; El-Temsah and Joner, 2013).

$$Fe^0 + O_2 + 2H \rightarrow Fe^{2+} + H_2O_2 \quad (1)$$

$$Fe^0 + H_2O_2 \rightarrow Fe^{2+} + 2OH^- \quad (2)$$

$$Fe^{2+} + H_2O_2 \rightarrow Fe^{3+} + OH^{\bullet} + OH^- \quad (3)$$

While NZVI toxicity may be mediated through ROS generation or through release of Fe^{2+}, it is reasonable to assume that close proximity of the NZVI to the bacteria would increase its toxicity potential. Prior reports of NZVI toxicity to *E. coli* have used uncoated NZVI which appears to have attached to the *E. coli* cell wall and the disruption of the cell membrane structures and increased membrane permeability were observed (Li et al., 2010; Zhou et al., 2014). TEM analysis allows visualized microstructure changes of *E. coli* due to the presence iron nanoparticles and therefore was employed to examine the NZVI or CNZVI treated *E. coli* cell (Fig. 3). Fig. 3a

showed a typical TEM image of native *E. coli*, which exhibited a well preservation of the cellular surface with distinct and coherent cytomembrane structure. Whereas a significantly difference from the control was that NZVI-treated cells partially dimmed outer boundary, reflecting harsh membrane damage and decomposition (Fig. 3b and c). The NZVI nanoparticles (i.e., the black dots) were clearly visible on the surface of cell block. Especially Fig. 3c demonstrates an accumulation of NZVI aggregates inside the cell, evidencing the cellular internalization of nanoparticles. However, in the case of CNZVI, the bacterial cell wall clearly displays an outer shell of a layer of nanoparticles attached around the outer membrane, while no cellular internalization of CNZVI was observed (Fig. 3d). Although the observation of CNZVI accumulation on the surface of *E. coli*, the CNZVI did not appear to destroy membrane integrity. It could be the reason that the large molecular weight polyelectrolytes (i.e., CMC) afford both an electrostatic and steric repulsion, known as electrosteric repulsion, inhibiting close contact between the particles and the cells.

In association with the stability tests in the previous section, the increasing concentration of CMC contributed to the higher stability of NZVI. Given the bare NZVI nanoparticles tend to aggregate to form micron-sized particles and thus may become less toxic, it was presumed that the more dispersed CNZVI particles may exert more significant cytotoxicity due to the inhibited particle aggregation. However, the results show that although the CMC stabilized the NZVI particles, reducing the aggregation and sedimentation, it inhibited the close contact between the NZVI particles and *E. coli* cells. This reveals the practicability of the use of the CMC as a stabilizer for NZVI in the practical environmental remediation.

3.3. Effect of Ca^{2+}

Previous studies have shown that the influences of ionic strength on the stability and mobility of the NZVI stabilized with different surface modifiers in water (He et al., 2007; Saleh et al., 2008; Dong and Lo, 2013b). The ionic strength and composition of the surrounding media may lead to aggregation or attraction of the NZVI particles to bacteria (Saleh et al., 2005, 2007). To gain insight into the mechanism of NZVI toxicity towards *E. coli*, additional inactivation experiments were performed in the presence of Ca^{2+} (Fig. 4). As demonstrated in Fig. 4a, the addition of 10 mg L^{-1} Ca^{2+} significantly reduced the inactivation of *E. coli* by NZVI. Previous study has found that the presence of Ca^{2+} can cause aggregation and sedimentation of NZVI by reducing the surface charge of NZVI and thus the repulsion among particles (Dong and Lo, 2013b). Zeta potential measurements were performed on the NZVI particles in the absence and presence of Ca^{2+} (Table 1). The NZVI particles exhibited a significant decrease in surface charge (from −20.1 mV to −4.7 mV) in the presence of 10 mg L^{-1} Ca^{2+}, which suggests that the electrostatic repulsion among particles reduced significantly. Thus it was presumed that the decreased toxicity towards *E. coli* might be ascribed to the enhanced aggregation of NZVI particles due to the presence of Ca^{2+}. However, it was interesting to find that the NZVI in the presence of 40 mg L^{-1} Ca^{2+} caused slightly higher toxicity than that at 10 mg L^{-1} Ca^{2+}. Zeta potential analysis demonstrates that the surface charge of NZVI particles reversed from negative charge to positive charge (4.4 mV) at 40 mg L^{-1} Ca^{2+}. This reveals that the positively charged NZVI particles became more favorable to adhere to the surface of negatively charged *E. coli* cells

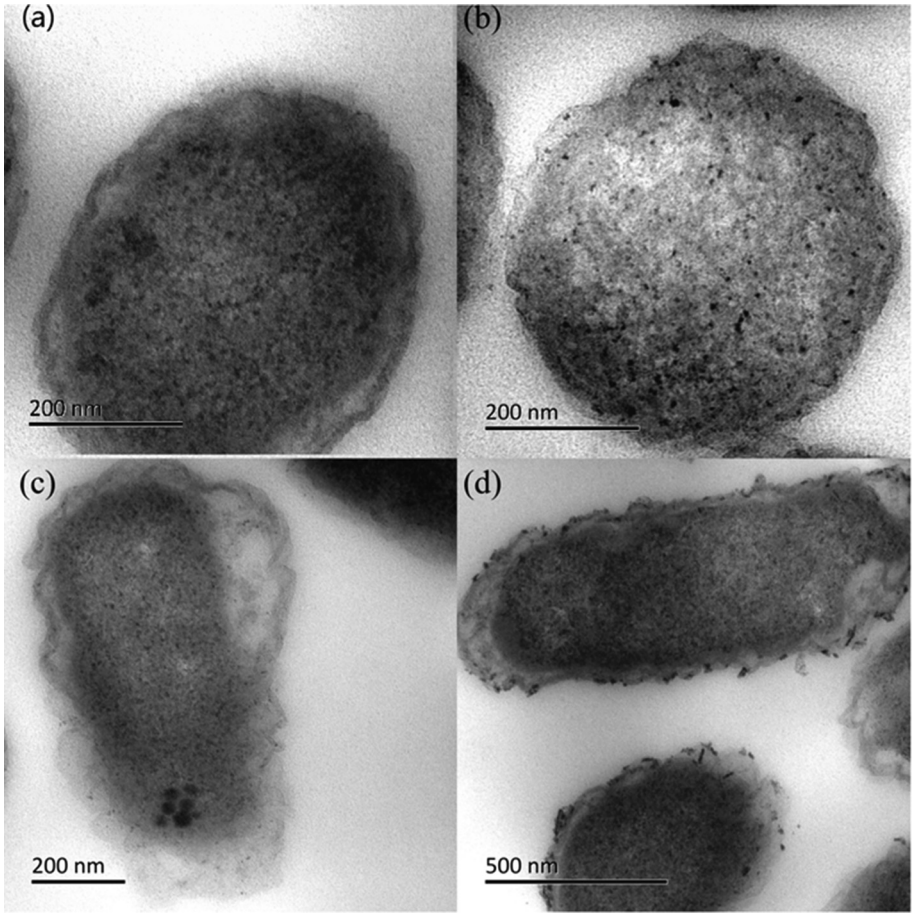

Fig. 3. Representative TEM pictures of (a) control and treated *E. coli* with (b, c) NZVI and (d) 0.4 wt% CNZVI for 1 h (Concentration of NZVI or CNZVI: 500 mg L^{-1}).

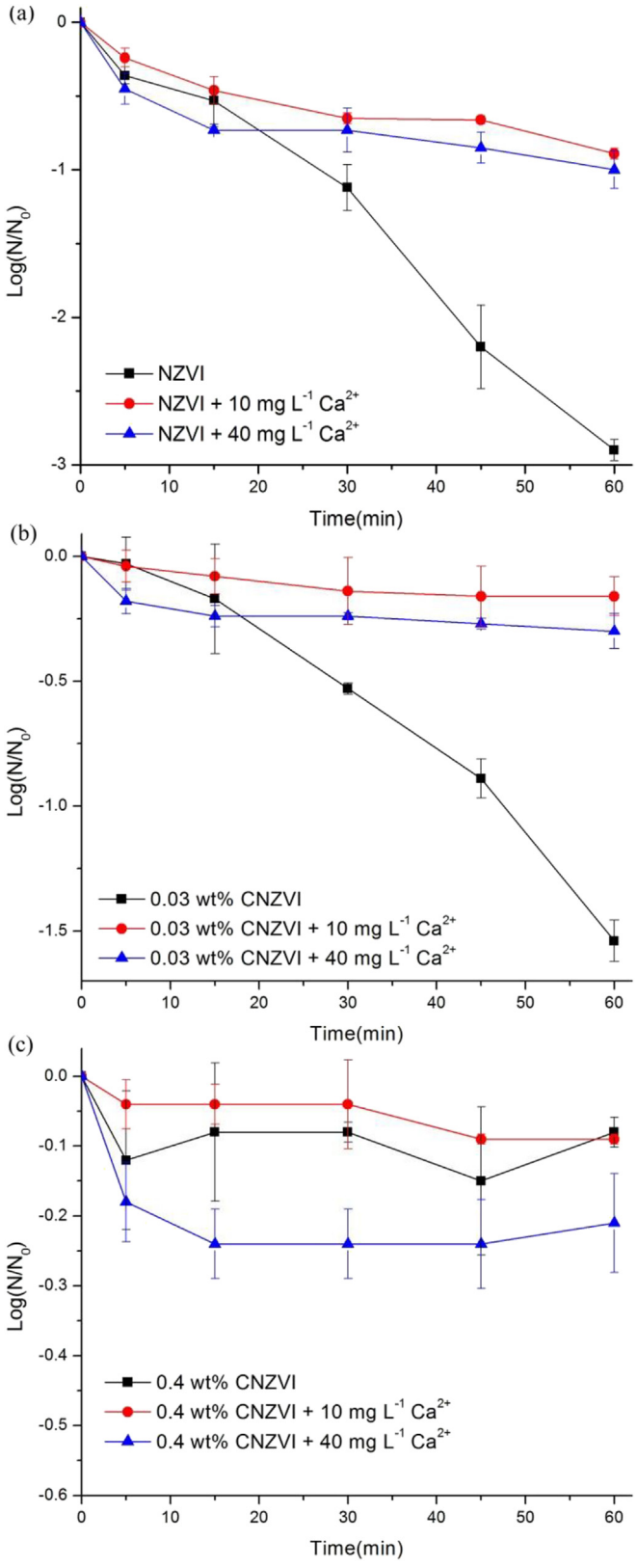

Fig. 4. Inactivation of *E. coli* by (a) NZVI, (b) 0.03 wt% CNZVI and (c) 0.4 wt% CNZVI in the absence or presence of Ca^{2+} (10 and 40 mg L^{-1}) (Concentration of NZVI or CNZVI: 500 mg L^{-1}).

(Chen et al., 2011a), which might have resulted in the increased toxicity. Besides, the Ca^{2+} might also act as a bridge between the negatively charged NZVI particles and the negatively charged *E. coli* cells, enhancing the particle attachment to *E. coli* cells. A similar effect of Ca^{2+} was observed for the 0.03 wt% CNZVI and 0.4 wt% CNZVI (Fig. 4b and c). Based on the above findings and discussions, it was concluded that Ca^{2+} might play a dual role in influencing the cytotoxicity of NZVI. On the one hand, the presence of Ca^{2+} can inhibit the bactericidal effect of NZVI by causing the aggregation and sedimentation of NZVI; on the other hand, the presence of Ca^{2+} may cause more serious toxicity by facilitating the adhesion of the NZVI particles onto the surface of bacteria.

3.4. Effect of aging treatment

The cytotoxicity of the aged NZVI and CNZVI nanoparticles (aged for 15 d and 30 d) were examined. As shown in Fig. 5, the log inactivation of *E. coli* after 1 h of treatment by the aged NZVI or CNZVI was significantly receded compared with the fresh iron nanoparticles. For the aged iron nanoparticles, just only the NZVI aged for 15 d still exhibited faint toxicity, resulted in a 0.32-log inactivation of *E. coli* within 60 min. As for the other aged nanoparticles, there were negligible toxicity effect (<0.15-log). This finding of decreased cytotoxicity of the aged NZVI is consistent with the findings of previous studies (Phenrat et al., 2009; El-Temsah and Joner, 2013; Fajardo et al., 2015). Phenrat et al. (2009) reported that the partial or complete oxidation of NZVI reduced its "redox" activity and thus the toxicity to mammalian cells. El-Temsah and Joner (2013) found that the adverse effects of NZVI on soil organisms seem temporary and reduced after oxidation. It was also reported the maintenance of cellular metabolism, the lack of oxidative stress and significant increase in cellular respiration in the soil treated by the aged NZVI (Fajardo et al., 2015).

Previous studies have revealed that the Fe^0 content and the dissolved Fe(II) contribute to the NZVI toxicity to *E. coli* (Auffan et al., 2008; Lee et al., 2008). In the presence of dissolved oxygen, it has been reported that the Fe^0 content of the particles was very rapidly consumed, and lepidocrocite (γ-FeOOH), magnetite and maghemite particles were the end products of this oxidation process (Kohn et al., 2005; Auffan et al., 2008; Reinsch et al., 2010; Liu et al., 2015). These different Fe-oxides may decrease adhesion to the cells, inhibit electron transfer due to the formation of Fe-oxides on the particle surface that are less conductive than magnetite, or lower the amount of Fe(II) adsorbed to or within in the surface

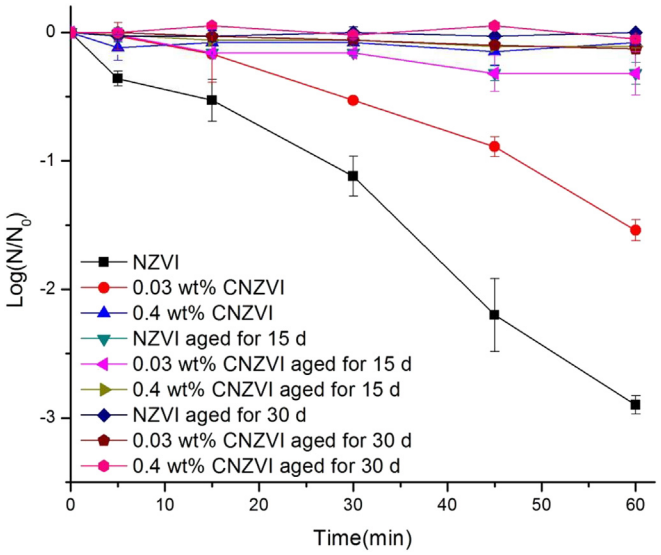

Fig. 5. Inactivation of *E. coli* by iron nanoparticles (500 mg L^{-1}) aged for 15 d and 30 d in the open air.

oxide (Reinsch et al., 2010) and therefore its toxicity to *E. coli*. The crystals and the elements of the fresh and aged NZVI and CNZVI particles were thus identified by XRD (Fig. 6). Fig. 6a shows the phase composition of fresh NZVI and CNZVI. The peaks at $2\theta = 45^\circ$ and 65° in both NZVI and CNZVI XRD pattern should be assigned to Fe^0 (Hoch et al., 2008). The other peaks as demonstrated in the CNZVI XRD pattern should be assigned to Na_2SO_4 (a residue from the synthetic process of CMC), which also indicates the successful coating of CMC on the surface of NZVI.

The XRD pattern of the iron nanoparticles aged for 15 and 30 d (Fig. 6b) indicated that the dominant oxide phase was magnetite (Fe_3O_4) or/and maghemite (γ-Fe_2O_3) for both NZVI and CNZVI. The magnetite and maghemite peaks are not differentiable because their lattice parameters are very similar (Williams and Scherer, 2001). In addition, small amounts of lepidocrocite (γ-FeOOH) can be identified in the XRD pattern of CNZVI aged for 15 d and the intensity of that further increased after 30 d of aging. Moreover, it was interesting to find that the intensity of Fe^0 peak in XRD pattern of NZVI aged for 15 d significantly decreased and disappeared after 30 d of aging, indicating the high degree of oxidation, while the Fe^0 peak still existed obviously in that of CNZVI aged for 15 d and 30 d. This reveals that the CMC coating might have influenced the process of oxidation. The other interesting finding is that the peaks assigned to Na_2SO_4 significantly decreased in the aged CNZVI. This may be resulted from the release of CMC coating from NZVI surface during the aging or due to the precipitation of iron oxides on the CNZVI surface, which covered the CMC coating. However, the effect of CMC on NZVI oxidation and the possibility of CMC release during aging were not further investigated, which will be the central objectives of future study. As discussed above, the magnetite or/and maghemite and lepidocrocite were the dominant oxide phases after aging, which has been reported less toxic or nontoxic to bacteria (Auffan et al., 2008; Chen et al., 2013; Zhou et al., 2014). The aged NZVI particles with no Fe^0 remaining had hardly any effect on *E. coli* cells. Even though the high content of Fe^0 still existed in the aged CNZVI, which did not cause any obvious toxic effect since the fresh CNZVI only exhibited slight toxicity towards *E. coli*.

4. Conclusions and implications

Herein, we discussed the dose-effect correlation of CMC stabilizer and NZVI in regard to the colloidal stability and toxicity of NZVI. It is found that CMC could not merely serve as a kind of excellent stabilizer but also inhibit NZVI's toxicity to *E. coli* largely. Furthermore, this study also examined the effect of Ca^{2+} on the toxicity of NZVI and CMC-modified NZVI (CNZVI) and it was found that Ca^{2+} might play a dual role in influencing the cytotoxicity of NZVI. On the one hand, the presence of Ca^{2+} decreased the toxic effect of NZVI by causing the aggregation and sedimentation of NZVI; on the other hand, the presence of Ca^{2+} might facilitate the adhesion of the NZVI particles onto the surface of bacteria, resulting in more serious cytotoxicity. The toxicity of the aged NZVI and CNZVI was also evaluated. The results show that the iron nanoparticles transformed to less-toxic or even nontoxic iron oxides, resulting in significant decrease in cytotoxicity.

Overall, these results could probably provide a reference for risk assessment for using NZVI particles for groundwater remediation and for using surface coatings on these nanoparticles. The unmodified NZVI particles would be oxidized in water and transform into the nontoxic magnetite and/or maghemite over months of aging, suggesting low risk to encountered ecosystems. Although surface modification increases NZVI's dispersion, it also appears to decrease its toxicity. However, since a variety of surface coatings which increase the colloidal stability and mobility of NZVI in aqueous phase are currently available, more efforts should be made to fully characterize their cytotoxicity.

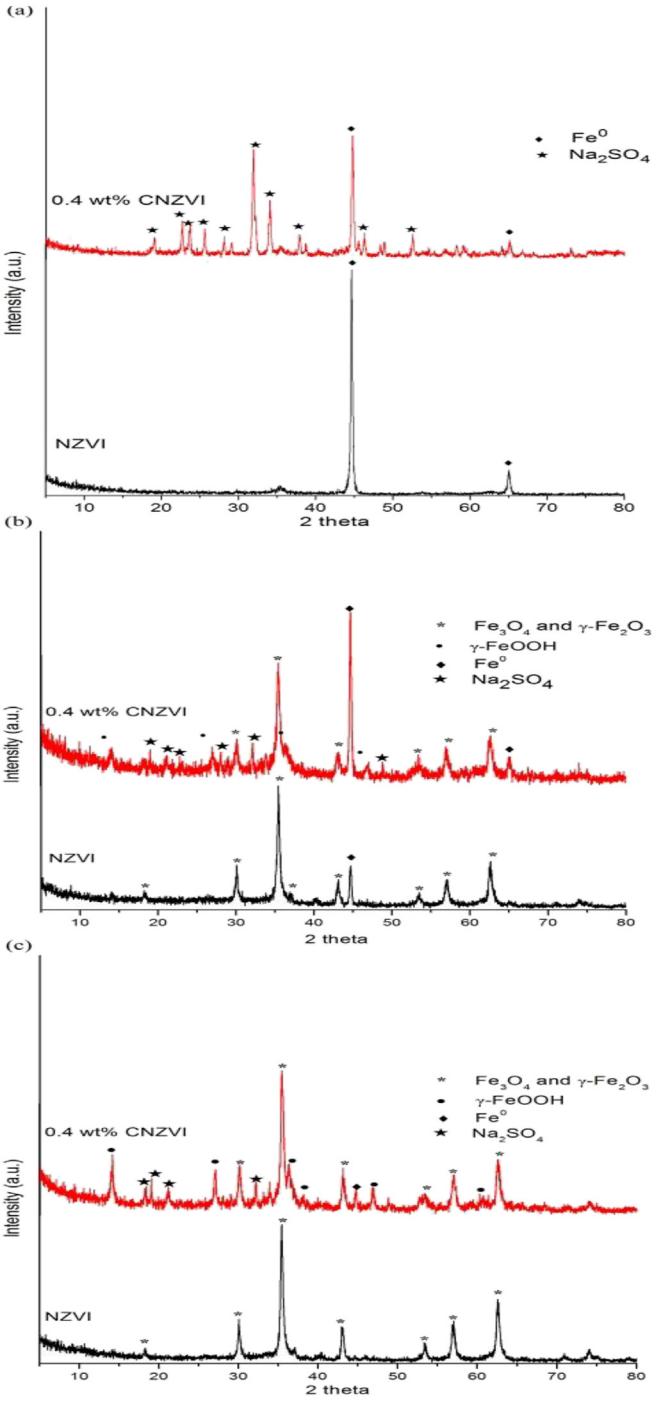

Fig. 6. XRD spectra of (a) freshly prepared iron nanoparticles (NZVI and 0.4 wt% CNZVI) and that of aged for (b) 15 d and (b) 30 d in the open air.

Acknowledgments

This research was supported by the Fundamental Research Funds for the Central Universities (531107040788), the National Natural Science Foundation of China (51409100, 51521006, 51378190) and the Program for Changjiang Scholars and Innovative Research Team in University (IRT-13R17). The authors also thank the NANOIRON® Company (Czech Republic, EU) for their

generous supply of the free NZVI samples.

References

Auffan, M., Achouak, W., Rose, J., Roncato, M.A., Chaneac, C., Waite, D.T., Masion, A., Woicik, J.C., Wiesner, M.R., Bottero, J.Y., 2008. Relation between the redox state of iron-based nanoparticles and their cytotoxicity toward Escherichia coli. Environ. Sci. Technol. 42, 6730–6735.

Chen, J., Xiu, Z., Lowry, G.V., Alvarez, P.J., 2011a. Effect of natural organic matter on toxicity and reactivity of nano-scale zero-valent iron. Water Res. 45, 1995–2001.

Chen, P.J., Su, C.H., Tseng, C.Y., Tan, S.W., Cheng, C.H., 2011b. Toxicity assessments of nanoscale zerovalent iron and its oxidation products in medaka (Oryzias latipes) fish. Mar. Pollut. Bull. 63, 339–346.

Chen, P.J., Tan, S.W., Wu, W.L., 2012. Stabilization or oxidation of nanoscale zerovalent iron at environmentally relevant exposure changes bioavailability and toxicity in medaka fish. Environ. Sci. Technol. 46, 8431–8439.

Chen, P.J., Wu, W.L., Wu, K.C., 2013. The zerovalent iron nanoparticle causes higher developmental toxicity than its oxidation products in early life stages of medaka fish. Water Res. 47, 3899–3909.

Dong, H., Guan, X., Lo, I.M., 2012. Fate of As(V)-treated nano zero-valent iron: determination of arsenic desorption potential under varying environmental conditions by phosphate extraction. Water Res. 46, 4071–4080.

Dong, H., Lo, I.M., 2013a. Influence of humic acid on the colloidal stability of surface-modified nano zero-valent iron. Water Res. 47, 419–427.

Dong, H.R., Lo, I.M.C., 2013b. Influence of calcium ions on the colloidal stability of surface-modified nano zero-valent iron in the absence or presence of humic acid. Water Res. 47, 2489–2496.

Dong, H., Lo, I.M.C., 2014. Transport of Surface-Modified Nano Zero-Valent Iron (SM-NZVI) in saturated porous media: effects of surface stabilizer type, subsurface geochemistry, and contaminant loading. Water Air Soil Pollut. 225 (9).

Dong, H.R., Zeng, G.M., Zhang, C., Liang, J., Ahmad, K., Xu, P., He, X.X., Lai, M.Y., 2015. Interaction between Cu^{2+} and different types of surface-modified nanoscale zero-valent iron during their transport in porous media. J. Environ. Sci. 32, 180–188.

El-Temsah, Y.S., Joner, E.J., 2013. Effects of nano-sized zero-valent iron (nZVI) on DDT degradation in soil and its toxicity to collembola and ostracods. Chemosphere 92, 131–137.

Fajardo, C., Gil-Diaz, M., Costa, G., Alonso, J., Guerrero, A.M., Nande, M., Lobo, M.C., Martin, M., 2015. Residual impact of aged nZVI on heavy metal-polluted soils. Sci. Total Environ. 535, 79–84.

Fajardo, C., Sacca, M.L., Martinez-Gomariz, M., Costa, G., Nande, M., Martin, M., 2013. Transcriptional and proteomic stress responses of a soil bacterium Bacillus cereus to nanosized zero-valent iron (nZVI) particles. Chemosphere 93, 1077–1083.

Fatisson, J., Ghoshal, S., Tufenkji, N., 2010. Deposition of carboxymethylcellulose-coated zero-valent iron nanoparticles onto silica: roles of solution chemistry and organic molecules. Langmuir 26, 12832–12840.

Grieger, K.D., Fjordboge, A., Hartmann, N.B., Eriksson, E., Bjerg, P.L., Baun, A., 2010. Environmental benefits and risks of zero-valent iron nanoparticles (nZVI) for in situ remediation: risk mitigation or trade-off? J. Contam. Hydrol. 118, 165–183.

He, F., Zhao, D., 2005. Preparation and characterization of a new class of starch-stabilized bimetallic nanoparticles for degradation of chlorinated hydrocarbons in water. Environ. Sci. Technol. 39, 3314–3320.

He, F., Zhao, D., Liu, J., Roberts, C.B., 2007. Stabilization of Fe-Pd nanoparticles with sodium carboxymethyl cellulose for enhanced transport and dechlorination of trichloroethylene in soil and groundwater. Ind. Eng. Chem. Res. 46, 29–34.

Hoch, L.B., Mack, E.J., Hydutsky, B.W., 2008. Carbothermal synthesis of carbon-supported nanoscale zero-valent iron particles for the remediation of hexavalent chromium. Environ. Sci. Technol. 42, 2600–2605.

Jiemvarangkul, P., Zhang, W.-x., Lien, H.-L., 2011. Enhanced transport of polyelectrolyte stabilized nanoscale zero-valent iron (nZVI) in porous media. Chem. Eng. J. 170, 482–491.

Jo, H.J., Choi, J.W., Lee, S.H., Hong, S.W., 2012. Acute toxicity of Ag and CuO nanoparticle suspensions against Daphnia magna: the importance of their dissolved fraction varying with preparation methods. J. Hazard Mater. 227–228, 301–308.

Joo, S.H., Feitz, A.J., Sedlak, D.L., Waite, T.D., 2005. Quantification of the oxidizing capacity of nanoparticulate zero-valent iron. Environ. Sci. Technol. 39, 1263–1268.

Kanel, S., Goswami, R., Clement, T., Barnett, M., Zhao, D., 2007. Two dimensional transport characteristics of surface stabilized zero-valent iron nanoparticles in porous media. Environ. Sci. Technol. 42, 896–900.

Kanel, S.R., Greneche, J.-M., Choi, H., 2006. Arsenic (V) removal from groundwater using nano scale zero-valent iron as a colloidal reactive barrier material. Environ. Sci. Technol. 40, 2045–2050.

Karn, B., Kuiken, T., Otto, M., 2009. Nanotechnology and in situ remediation: a review of the benefits and potential risks. Environ. health Perspect. 117, 1823–1831.

Kohn, T., Livi, K.J., Roberts, A.L., Vikesland, P.J., 2005. Longevity of granular iron in groundwater treatment processes: corrosion product development. Environ. Sci. Technol. 39, 2867–2879.

Lee, C., Kim, J.Y., Lee, W.I., Nelson, K.L., Yoon, J., Sedlak, D.L., 2008. Bactericidal effect of zero-valent iron nanoparticles on Escherichia coli. Environ. Sci. Technol. 42, 4927–4933.

Li, Z., Greden, K., Alvarez, P.J., Gregory, K.B., Lowry, G.V., 2010. Adsorbed polymer and NOM limits adhesion and toxicity of nano scale zerovalent iron to *E. coli*. Environ. Sci. Technol. 44, 3462–3467.

Lin, Y.H., Tseng, H.H., Wey, M.Y., Lin, M.D., 2010. Characteristics of two types of stabilized nano zero-valent iron and transport in porous media. Sci. Total Environ. 408, 2260–2267.

Liu, A., Liu, J., Zhang, W.X., 2015. Transformation and composition evolution of nanoscale zero valent iron (nZVI) synthesized by borohydride reduction in static water. Chemosphere 119, 1068–1074.

Lowry, G.V., 2007. Nanomaterials for Groundwater Remediation. McGraw-Hill, New York.

Phenrat, T., Long, T.C., Lowry, G.V., Veronesi, B., 2009. Partial oxidation ("aging") and surface modification decrease the toxicity of nanosized zerovalent iron. Environ. Sci. Technol. 43, 195–200.

Phenrat, T., Saleh, N., Sirk, K., Tilton, R.D., Lowry, G.V., 2007. Aggregation and sedimentation of aqueous nanoscale zerovalent iron dispersions. Environ. Sci. Technol. 41, 284–290.

Ramos, M.A., Yan, W., Li, X.-Q., Koel, B.E., Zhang, W.-X., 2009. Simultaneous oxidation and reduction of arsenic by zero-valent iron nanoparticles: understanding the significance of the core– shell structure. J. Phys. Chem. C 113, 14591–14594.

Raychoudhury, T., Tufenkji, N., Ghoshal, S., 2012. Aggregation and deposition kinetics of carboxymethyl cellulose-modified zero-valent iron nanoparticles in porous media. Water Res. 46, 1735–1744.

Reinsch, B.C., Forsberg, B., Penn, R.L., Kim, C.S., Lowry, G.V., 2010. Chemical transformations during aging of zerovalent iron nanoparticles in the presence of common groundwater dissolved constituents. Environ. Sci. Technol. 44, 3455–3461.

Sacca, M.L., Fajardo, C., Martinez-Gomariz, M., Costa, G., Nande, M., Martin, M., 2014. Molecular stress responses to nano-sized zero-valent iron (nZVI) particles in the soil bacterium Pseudomonas stutzeri. PloS One 9, e89677.

Sacca, M.L., Fajardo, C., Nande, M., Martin, M., 2013. Effects of nano zero-valent iron on Klebsiella oxytoca and stress response. Microb. Ecol. 66, 806–812.

Saleh, N., Kim, H.-J., Phenrat, T., Matyjaszewski, K., Tilton, R.D., Lowry, G.V., 2008. Ionic strength and composition affect the mobility of surface-modified Fe0 nanoparticles in water-saturated sand columns. Environ. Sci. Technol. 42, 3349–3355.

Saleh, N., Phenrat, T., Sirk, K., Dufour, B., Ok, J., Sarbu, T., Matyjaszewski, K., Tilton, R.D., Lowry, G.V., 2005. Adsorbed triblock copolymers deliver reactive iron nanoparticles to the oil/water interface. Nano Lett. 5, 2489–2494.

Saleh, N., Sirk, K., Liu, Y., Phenrat, T., Dufour, B., Matyjaszewski, K., Tilton, R.D., Lowry, G.V., 2007. Surface modifications enhance nanoiron transport and NAPL targeting in saturated porous media. Environ. Eng. Sci. 24, 45–57.

Schoonen, M.A.A., Cohn, C.A., Roemer, E., Laffers, R., Simon, S.R., O'Riordan, T., 2006. Mineral-induced formation of reactive oxygen species. Rev. Mineral. Geochem 64, 179–221.

Ševců, A., El-Temsah, Y.S., Joner, E.J., Černík, M., 2011. Oxidative stress induced in microorganisms by zero-valent iron nanoparticles. Microbes Environ. 26, 271–281.

Sirk, K.M., Saleh, N.B., Phenrat, T., Kim, H.-J., Dufour, B., Ok, J., Golas, P.L., Matyjaszewski, K., Lowry, G.V., Tilton, R.D., 2009. Effect of adsorbed polyelectrolytes on nanoscale zero valent iron particle attachment to soil surface models. Environ. Sci. Technol. 43, 3803–3808.

Tang, S.C., Lo, I.M., 2013. Magnetic nanoparticles: essential factors for sustainable environmental applications. Water Res. 47, 2613–2632.

Tiraferri, A., Chen, K.L., Sethi, R., Elimelech, M., 2008. Reduced aggregation and sedimentation of zero-valent iron nanoparticles in the presence of guar gum. J. Colloid Interf. Sci. 324, 71–79.

Williams, A.G., Scherer, M.M., 2001. Kinetics of Cr (VI) reduction by carbonate green rust. Environ. Sci. Technol. 35, 3488–3494.

Xiu, Z.M., Gregory, K.B., Lowry, G.V., Alvarez, P.J., 2010a. Effect of bare and coated nanoscale zerovalent iron on tceA and vcrA gene expression in Dehalococcoides spp. Environ. Sci. Technol. 44, 7647–7651.

Xiu, Z.M., Jin, Z.H., Li, T.L., Mahendra, S., Lowry, G.V., Alvarez, P.J., 2010b. Effects of nano-scale zero-valent iron particles on a mixed culture dechlorinating trichloroethylene. Bioresour. Technol. 101, 1141–1146.

Yin, K., Lo, I.M.C., Dong, H.R., Rao, P.H., Mak, M.S.H., 2012. Lab-scale simulation of the fate and transport of nano zero-valent iron in subsurface environments: aggregation, sedimentation, and contaminant desorption. J. Hazard. Mater 227–228, 118–125.

Zhou, L., Thanh, T.L., Gong, J., Kim, J.H., Kim, E.J., Chang, Y.S., 2014. Carboxymethyl cellulose coating decreases toxicity and oxidizing capacity of nanoscale zerovalent iron. Chemosphere 104, 155–161.